

FREQUENCY STABILIZATION IN AN ENCAPSULATED HIGH-Q MICROMECHANICAL RESONATOR VIA INTERNAL RESONANCE

Jun Yu¹, Hyun-Keun Kwon², Gabrielle D. Vukasin², Thomas W. Kenny² and Hanna Cho¹

¹The Ohio State University, Columbus, Ohio, USA and

²Stanford University, Stanford, California, USA

ABSTRACT

The frequency stability is a key parameter to determine the performance of a micro-electro-mechanical (MEM) resonator. In this study, we utilized the mechanism of 1:2 internal resonance (IR) in a hermetically encapsulated beam resonator with a high Q-factor (>4000) to improve the frequency stability. When a MEM resonator is driven by a single-frequency actuation and conditions for IR are satisfied, two engaged modes are simultaneously resonated with their phases locked together through a strong and effective intermodal energy transfer. The increased inertia of these two active resonant modes leads to the frequency stabilization in both frequency outputs. In an open-loop experimental setting, we demonstrated that the IR achieved a six-fold improvement in the frequency stability. This paper reports the first implementation of IR in an encapsulated high-Q beam resonator.

KEYWORDS

Micro-electro-mechanical resonator, internal resonance, frequency stabilization

INTRODUCTION

Micro-electro-mechanical systems (MEMS) attract great interest due to their compact dimensions, fast response, high sensitivity, and low power consumption, and are widely used in many industrial, commercial, and scientific applications [1]. MEM resonators are one category of MEMS that are designed to operate at or near their resonant frequencies. Because they are easy to integrate seamlessly with CMOS electronics and have diverse actuation/detection mechanisms, MEM resonators have been developed as a key element in MEM oscillators and sensors for providing reference frequencies and high sensitivity [2]. One of the most important attributes of resonators is the frequency stability, which determines their performance of sensitivity and reliability. However, when their dimensions shrink to micro- and even nanoscale, the frequency can fluctuate due to various noise sources even with tiny energy such as thermal noise, absorbing/desorbing molecules, and additive noises from actuation and transduction circuits [3]. Besides, especially for capacitive transduction with relatively low displacement sensitivity, the high driving power required to reach a detectable signal strength further degrades their frequency stability by introducing nonlinear behavior [4].

A recent report [5] shed light on the importance of mechanical domain in a MEM resonator as a main component inducing frequency fluctuations. By examining contributions of various noise sources on the resulting frequency stability, authors concluded that addressing the fluctuation of a mechanical resonator itself is essential to reach the ultimate thermomechanical noise limit. As such, we aim to improve stability of the mechanical resonator by

utilizing the mechanism of internal resonance (IR). IR can happen in a nonlinear system with its mode frequencies commensurate into an integer frequency ratio. In such a system, IR is triggered when the oscillation energy of the driven mode is larger than a critical value. Given all conditions of IR realized, the nonlinear coupling between the engaged modes can transfer energy effectively to induce these two (or more) modes into resonant states simultaneously [6-8]. From our previous analytical and experimental study [9], it was confirmed that a strong 1:2 or 2:1 IR between the second and third flexural modes could be achieved in a stepped-beam resonator. Such a strong IR mechanism can provide a stronger nonlinear energy transfer and wider IR operational range [7], compared to the relatively weaker 1:3 IR reported in [10]. In this previous study, however, the experimental demonstration was based on the laser vibrometry measurement on a low Q-factor resonator (~300), which did not reflect the practical conditions of a MEM resonator. In this paper, we fabricated a hermetically encapsulated beam resonator that was electrostatically actuated and detected, while the beam resonator was designed into a stepped beam with the dimensions required for the 1:2 frequency commensurability.

DEVICE DESCRIPTION AND OPERATION

To internally couple the second and third vibrational modes, the dimensions of a stepped-beam resonator (cf., Fig. 1a) were first determined to enforce a 1:2 ratio between these mode frequencies. A linear modal analysis

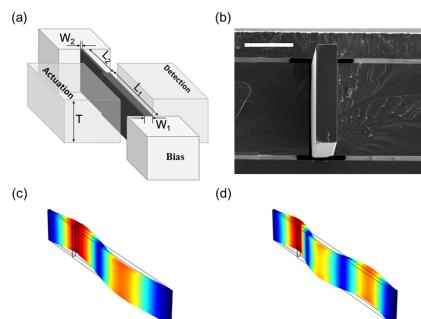


Figure 1: (a) Schematic of the micromechanical resonator and electrodes. The resonant beam vibrates in the flexural mode in the lateral direction (b) SEM image of the cross section of the resonator. The scale bar is 20 μ m. (c) FEA predicted mode shape of second mode with mode frequency of 1835kHz. (d) FEA predicted mode shape of third mode with mode frequency of 3671kHz.

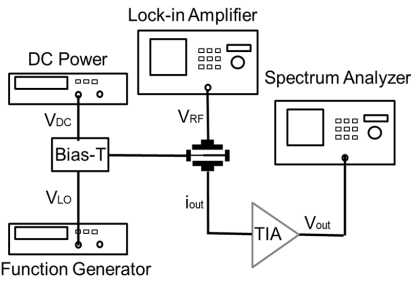


Figure 2: Schematic of RF/LO mixing measurement setup

was conducted by a commercial FEA software COMSOL on a doubly clamped stepped beam for various sets of width and length of the beam. The stepped beam with the dimensions of a wider part of $L_1=172\mu\text{m}$, $W_1=5\mu\text{m}$ and a narrower part of $L_2=50\mu\text{m}$, $W_2=3\mu\text{m}$ with a uniform thickness of $40\mu\text{m}$ gives the second and third mode frequencies of 1835kHz and 3671kHz , respectively, with their mode shapes shown in Figs. 1c-d. The devices were fabricated through Stanford-Bosch wafer-scale encapsulation process and a scanning electron microscopy (SEM) image on its cross-section is shown in Fig. 1b. The resonator and electrodes are sealed within its own vacuum chamber protecting the resonator from environmental disturbances. The advanced fabrication technique results in a high-quality structure to provide high Q-factor of fabricated resonators.

To operate the device in a straightforward way, a DC bias voltage was applied to a bias electrode, while an AC voltage was applied to an actuation electrode, resulting in an electrostatic force to actuate the beam in the lateral direction. The dynamic motion of beam, in turn, introduced a time-varying capacitance between the beam and detection electrode. Finally, the AC current including the motional signal was sensed from the output electrode by a transimpedance amplifier (TIA) to convert and amplify the current signal to a voltage signal.

In such a capacitive transduction, it is essential to eliminate the parasitic feedthrough capacitance that can mask the motional current. As such, we used a mixing measurement system, so called RF/LO measurement setup [11], as shown in Fig. 2. The lock-in amplifier provided a sweeping RF signal to the actuation electrode of system, while a local oscillator (LO) signal provided by a function generator was connected to the bias electrode via bias-T. The mixing of RF and LO signals results in a sinusoidal force with a frequency that equals to the frequency difference of RF and LO signals. When the frequency difference of RF and LO signals is set to be around the mode frequency (i.e., $\omega_{RF} - \omega_{LO} \approx \omega_0$), this sinusoidal force can be used to actuate the beam. Through the TIA, the output current was converted to an amplified voltage signal and measured by either a spectrum analyzer or a lock-in amplifier. The principle of this RF/LO mixing measurement is to circumvent parasitic feedthrough signal, because the parasitic signals exist on RF and LO frequencies rather than the frequency of driving force.

Here, the DC bias voltage can influence the mid-plane

stretching of beam and, thus, change its modal frequencies. By tuning the DC bias, we were able to reach or escape the IR range that satisfies the required 1:2 frequency commensurate condition between second and third flexural mode frequencies. We used this DC-tuning strategy to overcome fabrication variances in devices.

It is noted that the single global electrode design for actuation/detection electrodes was an inadequacy, because it was not ideal to actuate/detect higher flexural modes than the first mode. As the mode shape of the third flexural mode is one and a half sinusoids with two nodes along the electrode, only one third of the structure (half sinusoidal) can be effectively actuated/detected by the global electrode. This problem is even worse for the second mode. As a result, the actuation/detection scheme was not efficient as it was supposed to be, and thus there is more room for the result to be improved.

RESULTS

INTERNAL RESONANCE REALIZATION

We first experimentally characterized the mode frequencies and Q-factors of the first three flexural modes and compared them with the FEA simulation results, as summarized in Table 1. The experimentally obtained mode frequencies of first three flexural modes are very close to the ones estimated by FEA modal analysis. By tuning the DC bias to 22V, the ratio between the second and third flexural mode frequencies was achieved to be very close to 1:2. To verify if the IR was triggered, the drive frequency (Ω) was swept around the third mode frequency ($\sim 3.966\text{MHz}$) and the amplitudes of output signal were measured at the drive frequency (Ω) and one-half of the drive frequency (0.5Ω) simultaneously on the spectrum analyzer. As shown in Fig. 3, it was confirmed that the strong nonlinear energy transfer from the third to second mode happened to generate a strong IR peak around $\sim 1.983\text{MHz}$. Here, the third flexural mode was resonated by the external source (i.e., electrostatic force), while the second mode was resonated by the internal energy transfer. The internal energy exchange happened within a narrow frequency ranges $\sim 1.983\text{MHz}$ where the IR conditions were realized (i.e., 1:2 ratio and oscillation amplitude in the driven mode larger than a critical point), to reduce the amplitude of the driven mode (i.e., third mode) and increase the amplitude of the internally resonated mode (i.e., second mode).

Frequency stabilization

The inter-modal coupling of IR mechanism has a direct impact on frequency stability. When two modes are coupled and resonating with their phases locked together, the inertia of the mechanical domain, the tendency to remain at rest, increases and thus its fluctuation is reduced

Table 1. Comparison of mode frequencies between simulation and experiment

	1st mode	2nd mode	3rd mode
Experiment ($\omega_{oi}/2\pi$) [kHz]	716	1983	3966
Experiment (Q)	18000	6600	4100
Simulation ($\omega_{oi}/2\pi$) [kHz]	662	1835	3671

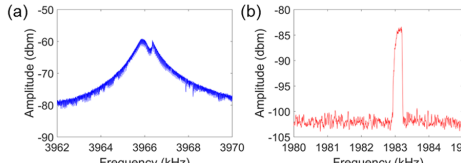


Figure 3: The system is driven near the third mode frequency (~ 3.966 MHz) by applying $V_{RF}=5V$, $V_{DC}=22V$, and $V_{LO}=10V$. The amplitudes of the output signal were measured at (a) the drive frequency and (b) at one-half of the drive frequency.

at the same energy level of noise. To experimentally verify frequency stabilization through the IR mechanism, we connect the output of TIA to a frequency counter and measure the open loop short-term frequency stability of the third mode up to 3000 seconds. The frequency fluctuation with IR is plotted in Fig. 4a and the frequency stability is estimated to be $\sqrt{\frac{1}{N-1} \sum_{i=1}^N \left(\frac{f_i - \bar{f}}{\bar{f}} \right)^2} = 11.9$ p.p.m. Then, we

tuned the DC bias to 5V, where the commensurate condition was no longer satisfied and IR was not triggered. In this case, the frequency stability of the third mode degraded to 68.1ppm and the frequency fluctuation increased as shown in Fig. 4b.

Open loop Allan deviations with IR and without IR are also plotted in Fig. 4c for $\sigma_y(\tau)$ expressed by:

$$\sigma_y(\tau) = \sqrt{\frac{1}{2(N-1)} \sum_{i=1}^{N-1} \left(\bar{y}_{i+1}^{\tau} - \bar{y}_i^{\tau} \right)^2}$$

where \bar{y}_i means the averaged frequency fluctuation during the i -th discrete time interval of τ . Note that these open loop Allan deviations cannot reflect the random walk of frequency. Because the phase locked loop (PLL) is not compatible with the RF/LO mixing setting and thus, we fixed the frequency of the driving signal. The Allan deviations for both cases continue decreasing with averaging time until they reach the limit of instrumentation rather than resonator itself. However, we can still compare the frequency fluctuation for both cases under same averaging time. Fig. 4c clearly shows the frequency fluctuation is stabilized by about an order when the IR is excited. By improving the experimental methodology, there is more room for the stability to be further improved by the closed-loop experiment.

CONCLUSION

We design and fabricate a batch of micromechanical resonators which can implement the IR. By controlling the DC bias, we achieve the commensurate relationship between second and third flexural modes, which is the prerequisite of IR. To experimentally characterize IR and study frequency stability, we setup a RF/LO mixing measurement system to avoid influence from the parasitic feedthrough current and acquire unmasked motional signal. In this setting, we verify that the IR happens in the stepped-beam resonator and its frequency stability improves by six-fold. The mechanism of IR stabilizes the frequency from the mechanical domain, which is the main source of frequency

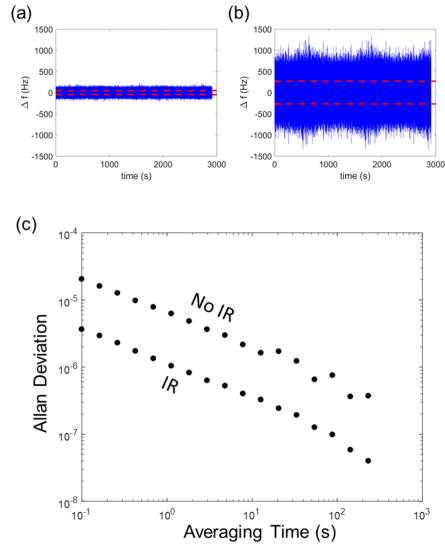


Figure 4: The short-term frequency fluctuation is plotted for 3000 seconds when the IR is triggered (a) and not triggered (b). The condition to realize the IR was controlled by tuning the applied DC bias. The frequency stability improved by 6 times from 68.1ppm to 11.9ppm. The Allan deviation with and without the IR in (c) also clearly shows the stability enhancement by an order.

fluctuation. Our study could enlighten further studies to address the frequency stability of MEMS oscillators and sensors from the mechanical domain to reach the ultimate thermo-mechanical noise limit.

ACKNOWLEDGEMENTS

This work was financially supported in part by Defense Advanced Research Projects Agency (Young Faculty Award D16AP00110). The contents of this paper are those of the authors and do not necessarily reflect the position or the policy of the government. This work is also supported by NSF Award # 1662464 - Collaborative Research: Nonlinear Coupling and Relaxation Mechanisms in Micro-mechanics. Special thanks to all the Stanford Nanofabrication Facility (SNF) staff for their help during fabrication.

REFERENCES

- [1] A. Z. Hajjaj, N. Jaber, S. Ilyas, F. K. Alfossail, and M. I. Younis, "Linear and nonlinear dynamics of micro and nano-resonators: Review of recent advances," *Int. J. Non-Linear Mech.*, Oct. 2019.
- [2] C. T. -c. Nguyen, "MEMS technology for timing and frequency control," *IEEE Trans. Ultrason. Ferroelectr. Freq. Control*, vol. 54, no. 2, pp. 251–270, Feb. 2007.
- [3] J. R. Vig and Yoonkee Kim, "Noise in microelectromechanical system resonators," *IEEE Trans. Ultrason. Ferroelectr. Freq. Control*, vol. 46, no. 6, pp. 1558–1565, Nov. 1999.

- [4] J. M. Miller, N.E. Bousse, D.B. Heinz, H.J.K. Kim, H.K. Kwon, G.D. Vukasin, and T.W. Kenny, "Thermomechanical-Noise-Limited Capacitive Transduction of Encapsulated MEM Resonators," *J. Microelectromechanical Syst.*, pp. 1–12, 2019.
- [5] M. Sansa, E. Sage, E.C. Bullard, M.Gely, T.Alava, E. Colinet, A.k. Naik, L.G. Villanueva, L. Duraffourg, M.L. Roukes and G. Jourdan "Frequency fluctuations in silicon nanoresonators," *Nat. Nanotechnol.*, vol. 11, no. 6, pp. 552–558, Jun. 2016.
- [6] A. Eichler, M. del Álamo Ruiz, J. A. Plaza, and A. Bachtold. "Strong coupling between mechanical modes in a nanotube resonator." *Physical review letters* 109, no. 2 (2012): 025503.
- [7] A.H. Nayfeh and D.T. Mook, "Nonlinear Oscillations," *John Wiley & Sons*, 2008
- [8] K. Asadi, J. Yu, and H. Cho, "Nonlinear couplings and energy transfers in micro- and nano-mechanical resonators: intermodal coupling, internal resonance and synchronization," *Philos. Trans. R. Soc. Math. Phys. Eng. Sci.*, vol. 376, no. 2127, p. 20170141, Aug. 2018.
- [9] J. Yu, K. Asadi, H. Brahmi, H. Cho, S. Nezmi, and S. Lee, "Frequency Stabilization in a MEMS Oscillator with 1:2 Internal Resonance," in *2019 IEEE International Symposium on Inertial Sensors and Systems (INERTIAL)*, 2019, pp. 1–4.
- [10] D. Antonio, D. H. Zanette, and D. López, "Frequency stabilization in nonlinear micromechanical oscillators," *Nat. Commun.*, vol. 3, no. 1, pp. 1–6, May 2012.
- [11] J. R. Clark, W.-T. Hsu, M. A. Abdelmoneum, and C. T.-C. Nguyen, "High-Q UHF micromechanical radial-contour mode disk resonators," *J. Microelectromechanical Syst.*, vol. 14, no. 6, pp. 1298–1310, Dec. 2005.

CONTACT

*J. Yu, tel: +1-929-2707662; yu.1768@osu.edu